HYDROGELS FOR CONTROLLED RELEASE OF ATROPINE IN CHEMICAL WARFARE AGENTS THREAT SCENARIOS

Adriana-Elena BRATU[1], Izabela-Cristina STANCU[2,*], Aurel DIACON[3], Gabriela TOADER[4], Ana Mihaela GAVRILA[5], Raluca Elena GINGHINA[6], Sebastian Stefan PRICOP[7], Tudor-Viorel TIGANESCU[8,*]

The influence of various functional additives (halloysite, β- and γ-cyclodextrins, TiO_2) on the properties and drug release behavior of photopolymerized semi-interpenetrating polymer network (sIPN)-PVA-based hydrogels was investigated. The sIPN hydrogels were characterized by SEM, FT-IR, mechanical tests (tensile, compression, and shear), and fluorescence-based release kinetics using atropine sulfate as a model drug. Results highlighted the role of these additives in tuning morphology, swelling behavior, mechanical and viscoelastic properties, and modulating non-Fickian release profiles of the semi-IPN hydrogels.

Keywords: hydrogel, drug release, halloysite, cyclodextrins, atropine sulfate, Non-Fickian diffusion

1. Introduction

Unfortunately, chemical terrorism has become one of the most serious threats to the modern world[1].Understanding the mechanism of action of these substances, as well as their toxicity, is important for the development of new technologies to combat them[2].Chemical warfare agents are banned compounds,

[1] PhD student, Faculty of Chemical Engineering and Biotechnologies, National University of Science and Technology POLITEHNICA Bucharest, and Research and Innovation Center for CBRN Defense and Ecology, Bucharest, Romania, e-mail: adriana.bratu@nbce.ro;
[2] Prof., Advanced Polymer Materials Group, National University of Science and Technology POLITEHNICA Bucharest, Bucharest, Romania, e-mail: izabela.stancu@upb.ro;
[3]Assoc. prof., PhD, Military Technical Academy „FERDINAND I", Bucharest, Romania, e-mail: aurel_diacon@yahoo.com;
[4] Assoc. prof., PhD, Military Technical Academy „FERDINAND I", Bucharest, Romania, e-mail: gabriela.toader@mta.ro;
[5] Researcher I, PhD, National Institute for Research, Development in Chemistry and Petrochemistry ICECHIM, Bucharest, Romania, e-mail: ana.gavrila@icechim.ro;
[6] Researcher III, PhD, Research and Innovation Center for CBRN Defense and Ecology, Bucharest, Romania, e-mail: raluca.ginghina@nbce.ro;
[7] Research Assistant, Research and Innovation Center for CBRN Defense and Ecology, Bucharest, Romania, e-mail: sebastian.pricop@nbce.ro;
[8] Prof., Military Technical Academy „FERDINAND I", Bucharest, Romania, e-mail: viorel.tiganescu@mta.ro

specifically developed to injure or kill in armed conflicts; they are extremely toxic and can be found in different forms – liquid, gas, or even solid[3]. Since 2011, chemical attacks have increased sharply, with chlorine, tear gas, and mustard gas being the most frequently used agents, while the use of sarin and cyanide has significantly declined[4].

Atropine, the most used antidote against nerve agents such as sarin and VX, blocks muscarinic receptors to reduce acetylcholine overload and prevent severe effects, including respiratory failure and bradycardia. While rapid injection is standard[5-7], controlled release formulations could sustain therapeutic levels over time, reducing the need for repeated dosing and enhancing protection during prolonged exposure[8-11].Controlled release of antidotes for nerve agent poisoning using hydrogels is a promising strategy to improve treatment and recovery. Atropine, also used in ophthalmology, can be efficiently released from β-cyclodextrin–functionalized hydrogels in a sustained manner [12, 13].

This study introduces novel hydrogel-based system for the controlled release of atropine, specifically designed for chemical warfare agents (CWA) threat scenarios, a concept not previously covered in the literature on sustained-release formulations of atropine. This approach proposes a simplified method for administering atropine as a therapeutic agent in scenarios involving CWA threats, focusing on the controlled release of atropine, an antidote for nerve agents[14] , as a model drug molecule, from various formulations of composite semi-interpenetrating polymer networks (sIPN) hydrogels involving inorganic adsorbents (halloysite nanoclay and TiO_2) and drug carrier/host molecule (cyclodextrins). Thus, novel sIPNs were obtained via the photopolymerization of 2-hydroxyethyl acrylamide (HEAA) and N-vinyl pyrrolidone (NVP) in the presence of polyvinyl alcohol, using triethylene glycol divinyl ether (DVE) as a crosslinking agent[15]. Subsequently, to improve the robustness and versatility of the hydrogel systems, specific additives (titanium dioxide - TiO_2, halloysite nanotubes[16], and β- and γ-cyclodextrins [17, 18]) were incorporated. TiO_2 nanoparticles and halloysite nanotubes primarily reinforced the hydrogel matrix and enhanced mechanical stability, while also influencing porosity and swelling behavior. In contrast, β- and γ-cyclodextrins were intended to facilitate host–guest interactions, thereby modulating the diffusion behavior and release kinetics of atropine.

2. Materials and Methods

a. Materials

Poly(vinyl alcohol) (PVA, average Mw 85,000-124,000, 87-89% hydrolyzed, Sigma Aldrich), halloysite – nanoclay (HNT, nanotube 30-70 nm × 1-3 μm, Sigma Aldrich), β –cyclodextrin (β-CD, ≥97%, Sigma Aldrich), γ –

cyclodextrin (γ-CD, ≥98%, Sigma Aldrich), titanium dioxide (TiO_2 nanoparticles ReagentPlus®, ≥99% Sigma Aldrich), N-vinyl pyrrolidone (NVP, 100 ppm sodium hydroxide as inhibitor, ≥99%, Sigma Aldrich), 2-hydroxyethyl acrylamide (HEAA, 1000 ppm monomethyl ether hydroquinone as stabilizer, 97%, Sigma Aldrich), tri(ethylene glycol) divinyl ether (DVE, 98%, Sigma Aldrich), 2-Hydroxy-4′-(2-hydroxyethoxy)-2-methylpropiophenone (Irgacure 2959, 98%, Sigma Aldrich), atropine sulfate (1 mg/mL injectable solution, Takeda), Phosphate buffered saline (PBS, pH 7.2-7.6, Sigma Aldrich) were used as received. Deionized water was freshly prepared in the laboratory and kept in tightly sealed containers to prevent contamination until the moment of use.

b. Methods

i. Synthesis of functionalized hydrogels for controlled release of atropine sulfate

Five novel hydrogels were obtained via the UV-induced free-radical photopolymerization of HEAA and NVP in the presence of PVA, using DVE as a crosslinking agent and various additives, as listed in Table 1. The aim of this research was to create systems that enable the incorporation and controlled release of atropine sulfate. Each formulation was tailored by introducing specific functional components: the use of titanium dioxide[19] or halloysite intended to improve mechanical resistance of the hydrogels[20], while β-cyclodextrin and γ-cyclodextrin, commonly used in pharmaceutical applications, aimed at facilitating the sustained release of active compounds[21]. The synthesis of each hydrogel formulation was performed by first dissolving 0.75 g of PVA in 15 mL of distilled water under magnetic stirring at 400 rpm overnight. Depending on the formulation (Table 1) additives such as halloysite, β-cyclodextrin, γ-cyclodextrin, or titanium dioxide were incorporated into the aqueous solution and were kept under magnetic stirring overnight. After complete dissolution, 3 g of NVP, 3.2 g of HEAA, and 0.56 g of DVE were added, and the solution was stirred at 450 rpm in the absence of light. Subsequently, 0.1 g of Irgacure 2959 (photoinitiator) were dissolved to obtain a homogeneous prepolymer mixture. The resulting mixture was then injected into glass molds (using different thickness rubber seals 2 mm for tensile testing and 4 mm for compression tests) under inert conditions to minimize oxygen inhibition. UV-induced photopolymerization was conducted using four cycles of individual side exposure (7 minutes each, with a 7 minutes pause in between). Temperature control was maintained using ice packs during pause period, the temperature of the molds not exceeding 40°C. The resulting hydrogel films were sectioned into rectangular strips for tensile (2×8×40 mm) and shear testing (2×10×10 mm), and into cylindrical specimens (Ø = 8mm× h = 4 mm) for compression testing, swelling behavior assessment, and evaluation of atropine sulfate loading and release capacity.

Table 1.

Hydrogel formulations designed for controlled atropine delivery

Component, (g)	Hydrogels				
	S_1	S_2	S_3	S_4	Bk
H_2O	15	15	15	15	15
PVA	0.75	0.75	0.75	0.75	0.75
Halloysite	0.25	0	0	0	0
β –cyclodextrin	0	0.25	0	0	0
γ – cyclodextrin	0	0	0.25	0	0
Titanium dioxide	0	0	0	0.022	0
NVP	3	3	3	3	3
HEAA	3.2	3.2	3.2	3.2	3.2
DVE	0.56	0.56	0.56	0.56	0.56
Irgacure 2959	0.1	0.1	0.1	0.1	0.1

ii. Loading atropine sulphate into the lyophilized hydrogels

Lyophilized hydrogels (Bk, S1, S2 and S3) were loaded with atropine sulfate by immersion in a 1 mg/mL aqueous solution, where diffusion ensured uniform impregnation of the sIPNs. Samples were incubated at 37 °C under 300 rpm agitation for 7 days to allow full penetration of the drug into the porous matrix. After loading, hydrogels were oven-dried at 50 °C for 4 days and stored in a desiccator. Constant weight was defined as mass stability to the fourth decimal place. The amount of loaded atropine was established from the remaining solution after loading, by fluorescence measurements and it was used as the maximum amount of atropine that could be released from each sample.

iii. Evaluation of the atropine sulfate release kinetics in PBS

The cumulative release of atropine sulfate is important in the therapeutic management of staff exposure to organophosphorus nerve agents[22]. Effective treatment requires the rapid and controlled delivery of the antidote, which can be supported by tunable hydrogel-based drug delivery systems. Atropine sulfate loading was achieved by immersing lyophilized hydrogels in aqueous solutions of known concentration, as described in the previous section. This enabled the gradual diffusion of the active substance into the polymer network, with the final loading efficiency influenced by structural parameters such as crosslinking density and porosity[23, 24]. The hydrogels loaded with atropine (approx. 110 mg) were placed in phosphate-buffered saline (10 mL) (pH 7.4) at 37 °C and 300 rpm using a reciprocating stirrer, for controlled release. Rehydration of the dried network enabled gradual drug release, influenced by crosslinking, porosity, temperature, and pH. Sampling (0.8 mL drown-up) was performed at regular intervals for UV-Vis and spectrofluorimetric analysis, replacing withdrawn volume with fresh PBS. Samples were protected from light to prevent atropine photodegradation. The evaluation was done in triplicate.

c. Characterizations

SEM imaging, which revealed the morphology of the lyophilized hydrogels, was performed using a Hitachi TM4000 Plus II SEM (15 kV, BSE mode). Prior to SEM analysis, samples were sputter-coated with a 5 nm gold layer using a Q150R ES Plus coater (Quorum Technologies, UK).

FT-IR analysis was performed on a Spectrum Two FTIR spectrometer (PerkinElmer) with a MIRacleTM Single Reflection ATR-PIKE Technologies at 4 cm^{-1} resolution, summing 32 scans in the 4000-550 cm^{-1} region.

To determine the gel fraction, an appropriate amount of the prepared hydrogel (w_h) was initially dried in the atmosphere, followed by further drying in a desiccator containing anhydrous $CaCl_2$ until a constant weight (w_d) was achieved. Subsequently, a specific quantity of the xerogel (w_d) underwent extraction in deionized water for 7 days, at room temperature, with daily water changes, and was then dried. This drying process consisted of an initial period in an oven at 50 °C for one week, followed by drying in a desiccator over anhydrous $CaCl_2$ until reaching a constant weight (w_e). The gel fraction (GF) was calculated by using equation (1): $GF\ (\%) = (w_e/w_d) \times 100$.

The swelling ratio of the hydrogel formulations designed for controlled atropine delivery was determined using the gravimetric technique[25], which involved immersing samples in DI water until they reached a constant weight at 37 °C. These swelling investigations were performed in duplicate, and the mean values for each sample were reported.

Uniaxial compressive tests were conducted at a rate of 2 mm/min using compression clamps with a diameter of 40 mm on a Discovery DMA 850 from TA Instruments. Five fully swollen disc specimens from each sample were subjected to compression on a stress ramp, and the mean values were reported. Tensile tests were also conducted to assess the mechanical resistance of hydrogels in uniaxial deformation at a rate of 2 mm/min. Five specimens from each sample were evaluated, and mean values were reported. Utilizing the same instrument, 'shear-sandwich' clamps were employed to evaluate the frequency-dependent shear modulus at a constant strain of 10% across a frequency range of 1 to 10 Hz. Additionally, the dependency of shear modulus on strain was investigated by ramping the strain from 10^0% to 10^2%, while maintaining a constant frequency of 10 Hz.

To evaluate the atropine release kinetics UV-Vis absorption intensity at 258 nm was measured for solutions containing atropine using a Jasco V550 spectrophotometer. Also, fluorescence intensity was measured at 283 nm using an excitation wavelength of 258 nm on a Jasco FP-6500 spectrofluorometer with 4mL fluorescence cuvettes. Calibration curves were established to accurately determine the concentration of atropine, the fluorescence-based method being established as offering the widest range and reproducible results (calibration curve Fig. 5a).

3. Results

SEM analysis (Fig. 1) revealed that the type of additive moderately influenced sample surface morphology, with variations in pore size and shape, distribution, and network organization. Samples containing cyclodextrins demonstrate structured, open porous architectures that have the potential to effectively support sustained drug release. In contrast, the hydrogel composites incorporating halloysite and TiO_2 present a fragmented, irregular network, which is probably suited for burst release. The reference hydrogel exhibited slightly looser and more irregular pores, compared to the cyclodextrins – based hydrogels. These findings suggest that additive selection plays an important role in tuning the morphology of hydrogels, which in turn may improve the effectiveness of drug delivery systems.

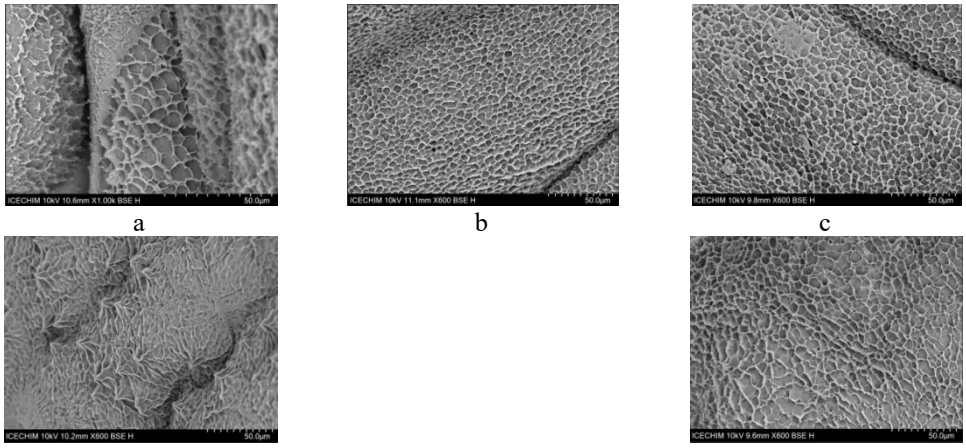

Fig. 1. SEM images of the morphology of the hydrogel formulations (a – S_1 - halloysite hydrogel, b – S_2 - β-cyclodextrin hydrogel, c – S_3 - γ-cyclodextrin hydrogel, d – S_4 - TiO_2 hydrogel, e – Bk - blank sample)

FT-IR analysis was performed to investigate the chemical structure of the synthesized hydrogel systems (Fig. 2). All samples exhibited broad bands at 3100–3500 cm^{-1}, corresponding to O–H stretching vibrations from PVA, HEAA, and inorganic additives. The intense peak near 1700 cm^{-1} was attributed to C=O stretching, while bands in the 1600–1500 cm^{-1} region indicated C=C and –NH deformations. Halloysite presence in S_1 was confirmed by Si–O–Si stretching at 1000–1100 cm^{-1}, and β-cyclodextrin in S_2 by C–O–C vibrations at 1150–1000 cm^{-1}. S_4 showed Ti–O vibrations (500–600 cm^{-1}), confirming TiO_2 incorporation. Despite these specific signals, the overall spectral profiles were similar due to the common polymer matrix (HEAA, NVP, DVE), with subtle differences in the fingerprint region indicating successful additive integration. The hydrogel

containing γ-cyclodextrin S_3 was excluded from the FT-IR multigraph due to the similarities with β-cyclodextrin in S_2.

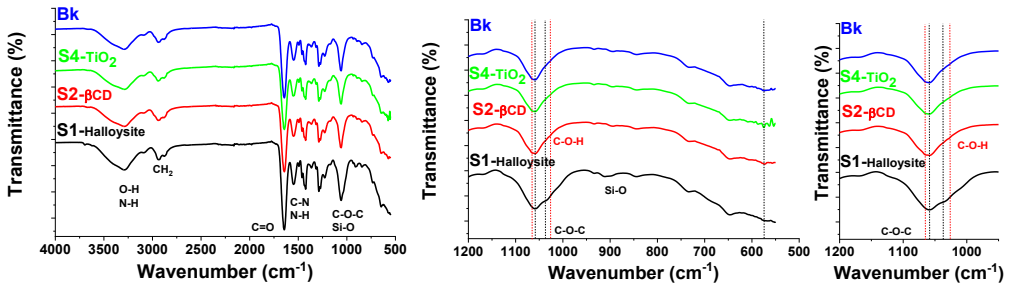

Fig. 2. FT-IR spectra of the hydrogel formulations and the blank

Fig. 3 a, b, c, d illustrate the equilibrium-swollen hydrogels along with gel fraction, conversion, and their swelling performances, respectively. All hydrogel formulations demonstrated high conversions and gel fractions. S1 reached the highest gel fraction value (90.85%), indicating a dense polymer network, and the lowest swelling ratio (7.9). In contrast, the other samples displayed higher swelling ratios (8.6-8.9). These results indicate that the halloysite acts as a reinforcing agent explaining both higher gel fraction and low swelling ratio.

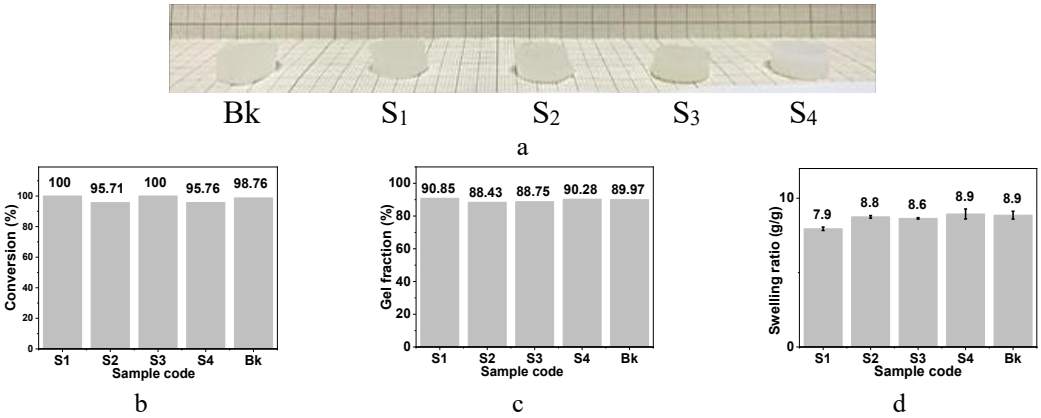

Fig. 3. (a) Equilibrium-swollen hydrogel discs; (b) Conversion; (c) Gel fraction;(d) swelling ratio

Thus, only halloysite had a more important effect on the swelling characteristics of the hydrogels, leading to a slightly lower swelling ratio, which can be attributed to a more efficient crosslinking since the gel fraction is also the highest for S1. This is explained by the participation of aluminosilicate in the crosslinking process through radical trapping by the hydroxyl groups on its surface.

The hydrogel containing γ-cyclodextrin (S_3) and the hydrogel containing β-cyclodextrin (S_2) displayed approximately equal gel fraction and swelling ratio.

The mechanical characterizations (Fig. 4) showed that hydrogel S_1 (halloysite hydrogel) had the highest tensile strength and rigidity, and the highest

storage modulus (G′), indicating a robust composite sIPN. Samples S_2 and S_3 (with β- and γ-cyclodextrins hydrogels) displayed high mechanical strength (tensile and compressive resistance) and also high G′ values, suggesting a flexible and stable sIPN hydrogel. In contrast, S_4 (TiO_2 hydrogel) and Bk (blank hydrogel) exhibited lower tensile and compressive resistance, the lowest G′ and higher G″, reflecting poor mechanical integrity and dominant viscous behavior. Since the sample containing TiO_2 exhibited irregular morphology and lower performance in terms of tensile and compression toughness, it was further excluded from the loading-release experiments.

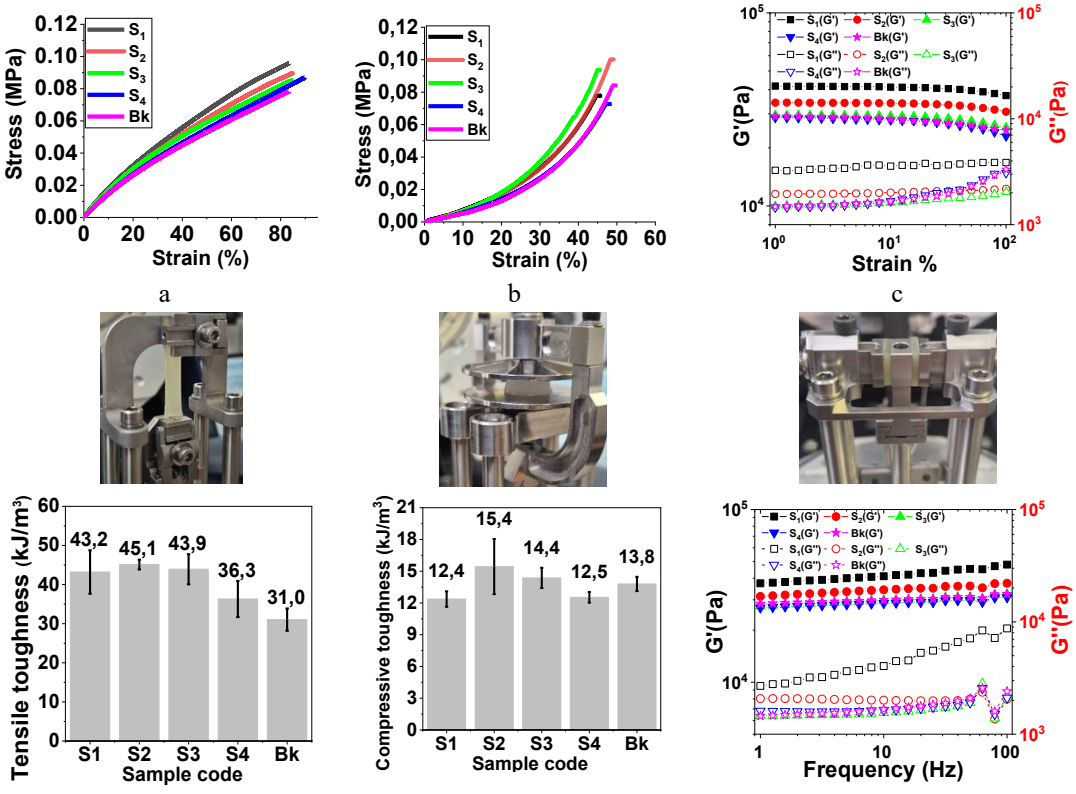

Fig. 4. Mechanical properties of the hydrogels: (a,d) tensile test; (b,e) compression test; (c,f) shear test

The release kinetics of atropine sulfate from four hydrogel formulations: S_1 (halloysite), S_2 (β-cyclodextrin), S_3 (γ-cyclodextrin), and Bk (blank hydrogel) were evaluated using zero-order, first-order, Higuchi, and Korsmeyer-Peppas models.

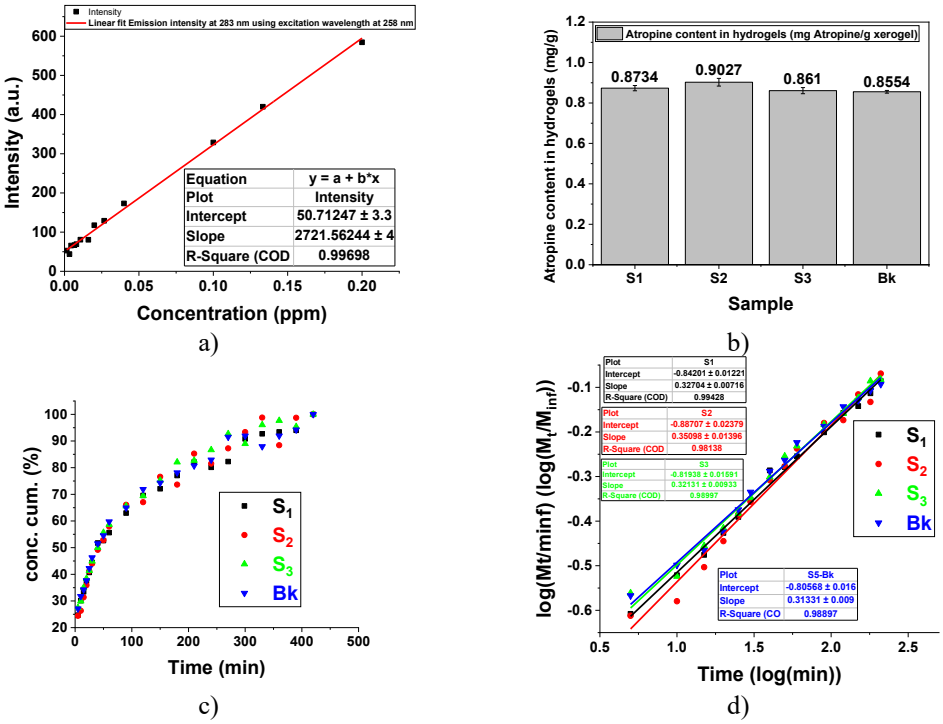

Fig. 5. a) Fluorescence calibration curve for atropine; b) Atropine sulfate amount loaded content in each hydrogel sample mg Atropine/g xerogel; c) Release profile in PBS of hydrogel samples loaded with atropine sulfate; d) Fitting of the release kinetics according to the Korsmeyer-Peppas model

All samples exhibited high correlation coefficients ($R^2 > 0.97$) for the Korsmeyer-Peppas model, indicating that diffusion is the dominant release mechanism (Fig. 5 d). Thus, the release of atropine sulfate from the hydrogels followed Korsmeyer–Peppas kinetics, with *n* values between 0.5–1 indicating non-Fickian diffusion [24, 26-28]. SEM analysis revealed that S_1 possessed the widest pore structure, while S_2 and S_3 displayed more compact morphologies, consistent with their more controlled release profiles. Although S_3 showed the highest zero-order release constant ($K_0 = 1.0134$ min^{-1}), suggesting a more uniform release rate, S_2 demonstrated a more favorable balance between release kinetics and structural control. Specifically, S_2 demonstrated a slightly higher diffusion exponent ($n = 0.3510$) in the Korsmeyer-Peppas model than S_3 ($n = 0.3217$). This suggests a slightly more intricate transport mechanism, which may involve additional polymer relaxation or interactions with the drug, rather than simple diffusion alone, potentially enhancing therapeutic modulation. Furthermore, β-cyclodextrin is known to form more stable inclusion complexes with atropine[29], potentially improving drug encapsulation and bioavailability. In contrast, the blank hydrogel (Bk) showed the lowest release constants, confirming the role of functional additives in enhancing drug delivery. Overall, the β-cyclodextrin hydrogel (S_2)

emerges as the most promising candidate for controlled therapeutic release of atropine sulfate, combining favorable kinetics, structural integrity, and molecular compatibility. The results from the loading and release experiments indicate that β-cyclodextrin hydrogel formulations could be a promising method for developing controlled drug delivery systems in both medical and defense applications. This is especially relevant for the sustained delivery of antidotes, such as atropine, in response to organophosphorus warfare agents threat scenarios.

Table 2.

Atropine sulfate release profiles from the synthesized hydrogels

The mathematical model	S_1	S_2	S_3	Bk
Zero-order	$Q\% = k_o t$			
K_0, min $^{-1}$	0.98	0.9933	1.0134	0.8317
R^2	0.8623	0.8861	0.8665	0.8369
First-order	$Q\% = 1 - e^{k_1 t}$			
K_1, min^{-1}	0.01042	0.01185	0.01038	0.008
A_1, min^{-1}	29.1352	27.1674	30.1100	32.3926
R^2	0.8365	0.8639	0.8816	0.8368
Higuchi	$Q\% = k_H t^{0.5}$			
K_H, min$^{-0.5}$	6.9387	6.4912	7.1295	6.5995
R^2	0.9799	0.9805	0.9799	0.9731
Korsmeyer-Peppas	$\log(Q\%) = \log(K) + n\log(t)$			
K_{KP}	0.1421	0.1297	0.15137	0.1564
R^2	0.9924	0.9814	0.9862	0.9899
n	0.3311	0.3510	0.3217	0.3133

6. Conclusions

We successfully developed by photopolymerizations IPN hydrogels, incorporating functional additives (halloysite, TiO_2, β- or γ-cyclodextrins), to regulate the release of atropine sulfate. FT-IR analysis confirmed the successful integration of the additives. The inclusion of halloysite notably enhanced mechanical strength and reduced swelling by generating a more compact polymer matrix while β- or γ-cyclodextrins led to hydrogels with high mechanical strength and also high G′ values, suggesting a flexible and stable sIPN hydrogel. The β-cyclodextrin-based hydrogel displayed the slowest release of the drug, likely due to optimal interactions between the atropine molecule and the hydrophobic cavity, facilitating strong host–guest interactions. Korsmeyer–Peppas modeling indicated that non-Fickian diffusion was the predominant mechanism driving atropine release, suggesting a combination of polymer relaxation and diffusion. These findings demonstrate that a careful selection of functional additives can finely tune both mechanical and drug delivery properties, highlighting the potential of sIPN hydrogels for targeted biomedical and defense applications.

Acknowledgments: This work was financially granted by the Ministry of Research, Innovation, and Digitalisation (UEFISCDI) by grants from the Ministry of Research, Innovation, and Digitization, CNCS UEFISCDI, project number PN-IV-P2-2.1-TE-2023-1293 - ctr. 40TE/2025, project number PN-IV-P7-7.1-PTE-2024-0305 - ctr. 40PTE/2025, project number PN-IV-P7-7.1-PED2024-0980 - ctr. 69PED/2025, within PNCDI IV, and project number PN-IV-P7-7.1-PTE-2024-0498 - ctr. 19PTE/2025.

R E F E R E N C E S

[1] *S. Zibasokhan, F. Teymouri, S. Sharififar, M. Azizi*. Factors Influencing the Integrated Management of Chemical Terrorist Incidents. Iranian Journal of War and Public Health, 16, (4), 2024, 309-317.

[2] *A.M.B. Amorim, L.F. Piochi, A.T. Gaspar, A.J. Preto, N. Rosário-Ferreira, I.S. Moreira*. Advancing Drug Safety in Drug Development: Bridging Computational Predictions for Enhanced Toxicity Prediction. Chem Res Toxicol, 37, (6), 2024, 827-849.

[3] *C.R. Jabbour, L.A. Parker, E.M. Hutter, B.M. Weckhuysen*. Chemical targets to deactivate biological and chemical toxins using surfaces and fabrics. Nature Reviews Chemistry, 5, (6), 2021, 370-387.

[4] *M.A. DeLuca, P.R. Chai, E. Goralnick, T.B. Erickson*. Five Decades of Global Chemical Terror Attacks: Data Analysis to Inform Training and Preparedness. Disaster Med Public Health Prep, 15, (6), 2021, 750-761.

[5] *D. Kobylarz, M. Noga, A. Frydrych, J. Milan, A. Morawiec, A. Glaca, et al.* Antidotes in Clinical Toxicology—Critical Review. Toxics, 11, (9), 2023, 723.

[6] *R.J. Geller, G.P. Lopez, S. Cutler, D. Lin, G.F. Bachman, S.E. Gorman*. Atropine availability as an antidote for nerve agent casualties: validated rapid reformulation of high-concentration atropine from bulk powder. Ann Emerg Med, 41, (4), 2003, 453-456.

[7] *M.J. Rodríguez Fernández, D. Hernández, B.J. Anaya, D.R. Serrano, J.J. Torrado*. Stability of Multicomponent Antidote Parenteral Formulations for Autoinjectors against Chemical War Agents (Neurotoxics). Pharmaceutics, 16, (6), 2024, 820.

[8] *G. RamaRao, P. Afley, J. Acharya, B.K. Bhattacharya*. Efficacy of antidotes (midazolam, atropine and HI-6) on nerve agent induced molecular and neuropathological changes. BMC Neuroscience, 15, (1), 2014, 47.

[9] *Y. He, S. Zeng, A.M. Abd El-Aty, A. Hacımüftüoğlu, W. Kalekristos Yohannes, M. Khan, et al.* Development of Water-Compatible Molecularly Imprinted Polymers Based on Functionalized β-Cyclodextrin for Controlled Release of Atropine. Polymers, 12, (1), 2020, 130.

[10] *M. Parrot, B. Yathavan, O. Averin, L. Hoggard, J.E. Rower, M. Voight, et al.* Clinical pharmacokinetics of atropine oral gel formulation in healthy volunteers. Clin Transl Sci, 17, (3), 2024, e13753.

[11] *P. Garg, P. Shokrollahi, H.F. Darge, C.M. Phan, L. Jones*. Controlled PVA Release from Chemical-Physical Interpenetrating Networks to Treat Dry Eyes. ACS Omega, 10, (1), 2025, 1249-1260.

[12] *Z.L. Wang, Ting; Li, Xinhua; Wu, Haitao; Li, Yuhang; Hao, Lingyun*. Preparation of Molecularly Imprinted Hydrogel Contact Lenses for Extended Atropine Eluting. Journal of Biomedical Nanotechnology, 19, (5), 2023, 804-813(810).

[13] *K.-Y. Wong, Y. Liu, C.-M. Phan, L. Jones, M.-S. Wong, J. Liu*. Selection of DNA aptamers for sensing drugs treating eye disease: atropine and timolol maleate†‡†The authors have filed

patent related to this work.‡Electronic supplementary information (ESI) available. See DOI: https://doi.org/10.1039/d4sd00223g. Sensors and Diagnostics, 3, (10), 2024, 1679-1688.

[14] *K. Feng, J.A. Zhang, W.T. Shen, T. Leng, Z. Zhou, Y. Yu, et al.* Recent Development of Nanoparticle Platforms for Organophosphate Nerve Agent Detoxification. Langmuir, 41, (4), 2025, 2124-2140.

[15] *H. Shu, P. Chen, R. Yang*. Advances in Antibacterial Polymer Coatings Synthesized via Chemical Vapor Deposition. Chem & Bio Engineering, 1, (6), 2024, 516-534.

[16] *F.B. Alakija, D.K. Mills*. Fabrication and Characterization of a Stretchable Sodium Alginate Hydrogel Patch Combined with Silicon Nitride and Metalized Halloysite Nanotubes to Develop a Chronic Wound Healing Treatment. International Journal of Molecular Sciences, 26, (4), 2025, 1734.

[17] *J. Liu, B. Tian, Y. Liu, J.B. Wan*. Cyclodextrin-Containing Hydrogels: A Review of Preparation Method, Drug Delivery, and Degradation Behavior. Int J Mol Sci, 22, (24), 2021.

[18] *H. Omidian, A. Akhzarmehr, E.J. Gill*. Cyclodextrin–Hydrogel Hybrids in Advanced Drug Delivery. Gels, 11, (3), 2025, 177.

[19] *P.P. Nayak, S. Kini, K. Ginjupalli, D. Pai*. Effect of shape of titanium dioxide nanofillers on the properties of dental composites. Odontology, 111, (3), 2023, 697-707.

[20] *M. Mrówka, M. Szymiczek, T. Machoczek, M. Pawlyta*. Influence of the Halloysite Nanotube (HNT) Addition on Selected Mechanical and Biological Properties of Thermoplastic Polyurethane. Materials, 14, (13), 2021, 3625.

[21] *O.E. Nicolaescu, I. Belu, A.G. Mocanu, V.C. Manda, G. Rău, A.S. Pîrvu, et al.* Cyclodextrins: Enhancing Drug Delivery, Solubility and Bioavailability for Modern Therapeutics. Pharmaceutics, 17, (3), 2025.

[22] *J. Kassa, C.M. Timperley, M. Bird, A.C. Green, J.E.H. Tattersall*. Influence of Experimental End Point on the Therapeutic Efficacy of Essential and Additional Antidotes in Organophosphorus Nerve Agent-Intoxicated Mice. Toxics, 10, (4), 2022, 192.

[23] *N. Nassar, S. Kasapis*. Fundamental advances in hydrogels for the development of the next generation of smart delivery systems as biopharmaceuticals. International Journal of Pharmaceutics, 633, 2023, 122634.

[24] *S. Erikci, N. van den Bergh, H. Boehm*. Kinetic and Mechanistic Release Studies on Hyaluronan Hydrogels for Their Potential Use as a pH-Responsive Drug Delivery Device. Gels, 10, (11), 2024, 731.

[25] *C.M. Ninciuleanu, R. Ianchiş, E. Alexandrescu, C.I. Mihăescu, C. Scomoroşcenco, C.L. Nistor, et al.* The Effects of Monomer, Crosslinking Agent, and Filler Concentrations on the Viscoelastic and Swelling Properties of Poly(methacrylic acid) Hydrogels: A Comparison. Materials, 14, (9), 2021, 2305.

[26] *P. Rattanaseth, K. Katewongsa, K. Intuyod, S. Pinlaor, R. Thanan, C. Sakonsinsiri*. Poly(d,l-lactide-co-glycolide) Nanoparticles Encapsulating Doxorubicin for Improved Treatment in Cholangiocarcinoma and Drug-Resistant Cells. ACS Applied Bio Materials, 8, (7), 2025, 6055-6065.

[27] *R. Dwivedi, A.K. Singh, A. Dhillon*. pH-responsive drug release from dependal-M loaded polyacrylamide hydrogels. Journal of Science: Advanced Materials and Devices, 2, (1), 2017, 45-50.

[28] *M. Vigata, C. Meinert, D.W. Hutmacher, N. Bock*. Hydrogels as Drug Delivery Systems: A Review of Current Characterization and Evaluation Techniques. Pharmaceutics, 12, (12), 2020.

[29] *M. Butnariu, M. Peana, I. Sarac, S. Chirumbolo, H. Tzoupis, C.T. Chasapis, et al.* Analytical and in silico study of the inclusion complexes between tropane alkaloids atropine and scopolamine with cyclodextrins. Chemical Papers, 75, (10), 2021, 5523-5533.